

Classification of nutrient deficiency in oil palms from leaf images using convolutional neural network

Muhammad Ikmal Hafiz Razali¹, Muhammad Asraf Hairuddin², Aisyah Hartini Jahidin³, Mohd Hanafi Mat Som⁴, Megat Syahirul Amin Megat Ali⁵

¹Mindmatics Sdn. Bhd., Kajang, Malaysia

²College of Engineering, Universiti Teknologi MARA Cawangan Johor, Kampus Pasir Gudang, Masai, Malaysia

³Centre for Foundation Studies in Science, University of Malaya, Kuala Lumpur, Malaysia

⁴Faculty of Electronic Engineering Technology, Universiti Malaysia Perlis, Arau, Malaysia

⁵Microwave Research Institute, Universiti Teknologi MARA, Shah Alam, Selangor, Malaysia

Article Info

Article history:

Received Sep 22, 2021

Revised Jun 15, 2022

Accepted Jul 14, 2022

Keywords:

Convolutional neural network

Leaf images

Nitrogen deficiency

Oil palm

Potassium deficiency

ABSTRACT

Oil palm is a perennial plant that thrives well in tropical climate. Apart from humid environment, the plant also requires a wide variety of nutrients. Any deficiencies will directly affect its growth and palm oil production. These can often be detected from the change of leaf colour and texture. Deviations from the standard dark green colour indicates lack of certain nutrients. Therefore, this study proposes convolutional neural network (CNN) to classify nutrient deficiency in oil palms using leaf images. A total of 180 leaf images are acquired using standardized protocol. The samples are evenly distributed into healthy, nitrogen-deficient, and potassium-deficient groups. Residual network (ResNet)-50, visual geometry group-16 (VGG-16), Densely connected network (DenseNet)-201, and AlexNet are trained and tested using the randomized samples. Each attained classification accuracies of 96.7%, 100%, 98.3%, and 100% respectively. Despite yielding similar performance, AlexNet is the more computational efficient architecture with less convolutional layers compared to VGG-16.

This is an open access article under the [CC BY-SA](https://creativecommons.org/licenses/by-sa/4.0/) license.



Corresponding Author:

Megat Syahirul Amin Megat Ali

Microwave Research Institute, Universiti Teknologi MARA

40450 Shah Alam, Selangor, Malaysia

Email: megatsyahirul@uitm.edu.my

1. INTRODUCTION

Oil palm (*Elaeis guineensis*) was first introduced in Malaysia as an ornamental plant [1]. However, due to its widespread commercial value, the oil palm is grown in large scale plantation estates. The plantation area grew from 1.5 million hectares in 1985 to 4.7 million hectares in 2009. This shows the significant contribution of oil palm to the economy and has since become an important commodity crop for the country [2]. Currently, Malaysia is the second largest producer of palm oil in the world and provides 38% of the global supply. The production has increased steadily over the years, reaching 39.04 million tons in 2011 alone. The industry easily meets the local demand for oil and fat, and the surplus is exported overseas. Manufacturers have also invested in the post-processing of palm oil to ensure efficient refining and fractionation process [1]. However, the growth of oil palm also contributes to the amount and quality of oil yield. Hence, monitoring of the plant during the early phase of growth is equally important.

The perennial plant grows well in tropical climate and is highly productive under the appropriate environment conditions [3]. Oil palm requires a variety of nutrients such as nitrogen, potassium, phosphorus, magnesium, boron, copper, and zinc for optimum growth and productive yield [4]. Nutrient deficiency can be

detected at early stage of growth. This can be physically observed from the characteristics of the trunk and leaves. Oil palm that lacks phosphorus will result in a trunk structure that is narrow and tapered [5]. Meanwhile, deficiency of specific nutrients such as nitrogen and potassium can be observed from the leaves. Healthy oil palms have dark green leaflets, with strong and flexible characteristics. Conversely, nitrogen-deficient plants can be detected from light green- and yellow-coloured leaves. Lack of potassium is indicated by confluent orange spotting on the leaflets [6].

The evaluation is subjective and performed by trained operators [7]. To address this limitation, a computerized system that assess nutrient deficiencies from leaf images is required. These images can be fed to deep learning algorithms for extracting intrinsic information related to specific nutrient deficiency. The method imitates the human brain in generalizing solution from new experience [8]. Deep learning allows machines to solve complex problems even from diverse and unstructured data. The technique requires less data pre-processing than the more primitive architectures. Theoretically, a deeper structure should result in improved performance compared to shallower network structure [9]. The method can generally be segregated based on the type of data being used. While the long short-term memory (LSTM) network specifically caters for time-series information [10], convolutional neural network (CNN) is developed for image recognition [11].

Various pre-trained CNN structures are readily available and new models can be built to enhance the existing network. These include the residual network (ResNet) [12], visual geometry group network (VGGNet) [13], densely connected network (DenseNet) [14], and AlexNet [15]. Each of these differ in the number of deep layers involved. Comparatively, report has been conflicting on the best performing architectures. Several literatures claimed DenseNet [16], [17], while others highlighted AlexNet [18], [19] as the better alternative. Therefore, it is assumed that the performance is dependant on the problem and parameters being studied. Another parameter to be considered when assessing the performance is computational cost which is proportional to the number of convolutional layers [20]. Generally, these CNN structures have been successfully implemented in agriculture for monitoring agriculture areas based on satellite images [21], prediction of crop yield [22], fruit counting [23], weed and crop recognition [24], leaf stress [25] and diseases [19], as well as detection of post-harvest pesticide residue [26]. CNN has also been applied to detect multiple plant diseases from leaf image with excellent classification accuracy [17]. Therefore, this highlights the potential of CNN for classifying nutrient deficiency in oil palms from the leaf images.

Based on the extensive review, two major gaps in the literature have been identified. First, a standardized protocol for the acquisition of leaf images is needed. This involve investigating suitable positioning of the camera, lighting, and uniformed background upon which the leaves will be placed against. Second, CNN has never been implemented for classifying nutrient deficiency from the leaf images. Several architectures can thus be evaluated for the best classification performance and computational efficiency. therefore, the study sets out to achieve the following objectives: i) To establish image acquisition protocol, and ii) to develop and assess CNN architectures for classifying nutrient deficiency from the leaf images. The study is significant as untrained operators can perform objective assessment on the nutrition status of oil palms through image acquisition protocol and deep learning classification model.

2. RESEARCH METHOD

Generally, the study sets out to solve two major objectives. The image acquisition protocol is first standardized. Subsequently, the leaf images are acquired based on the predefined procedure. Image samples are then segregated into healthy, nitrogen-deficient, and potassium-deficient groups. The data is randomized and next, partitioned for network training and testing. The classification model is then developed based on ResNet, VGGNet, DenseNet and AlexNet architectures. Consequently, the individual network is evaluated based on the best classification performance and computational efficiency. Figure 1 illustrates the general framework of research methods.

2.1. Protocol and acquisition of leaf images

Initially, a suitable image acquisition protocol is standardized prior to the actual data collection. As shown in Figure 2, the leaves sampled from the oil palm is placed against a black background to avoid reflection of incoming light source. A camera with light source unit is placed 8 centimeters (cm) from the sample. A smartphone with 12 megapixels (MP) camera is sufficient to capture the leaf characteristics at great level of detail. Leaf samples are acquired from a plantation at Taman Tualang Indah, Temerloh, Pahang. The location is selected as the oil palms are still in the early growth phase. Therefore, the leaves can be obtained by cutting them from the main branch. The operators can periodically assess the plant conditions through visual observation of the leaf characteristics. These are based on subjective evaluations and the assessment varies from one individual to another. The dataset is segregated into the healthy controls, nitrogen-deficient, and potassium-deficient groups.

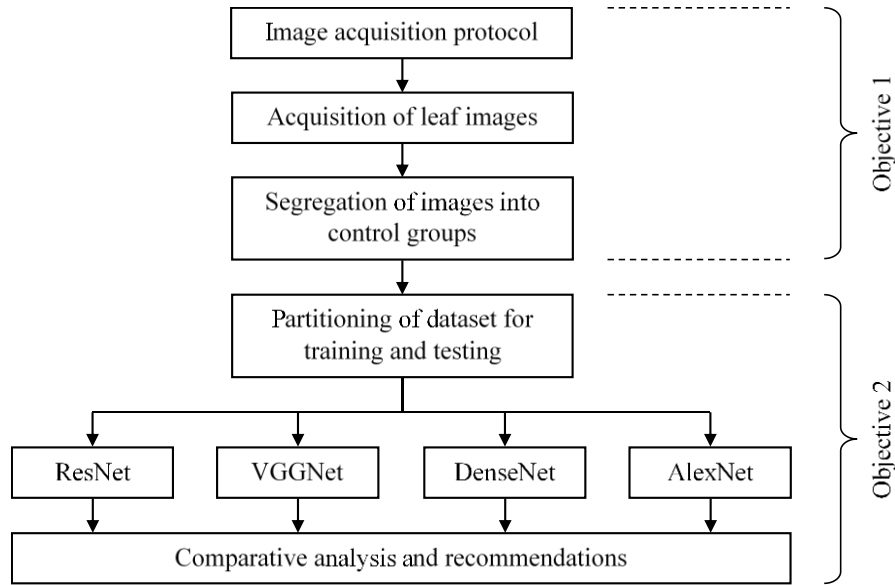


Figure 1. Framework of research methods

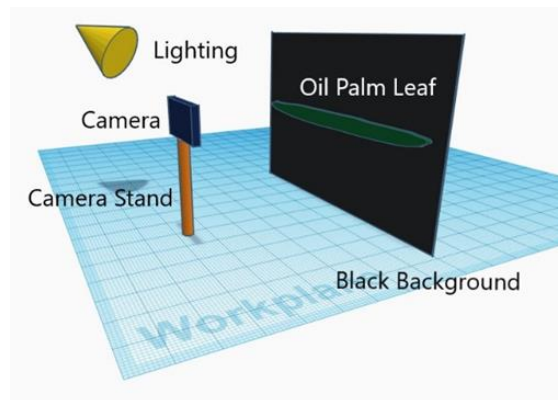


Figure 2. Image acquisition setup

2.2. Convolutional neural network

All image classification tasks using CNN are performed in matrix laboratory (MATLAB). CNN is comprised of four major components: the convolution layer, activation functions, pooling, and fully connected layers. The original $3,456 \times 3,456$ pixels images are resized using zero-center normalization method and makes use of the red-green-blue (RGB) channels. Normalization is required as it avoids gradient explosion in accelerated network convergence. These further reduces the number of feature maps [27]. Learnable filters are used by the convolutional layer to detect specific patterns from the input. The filter is slid across the area of the image and a dot product is computed to obtain an activation map. Rectified linear unit (ReLU) is implemented as the activation function in the convolutional layer as it does not activate all neurons simultaneously and thus, improves computational efficiency. Meanwhile, softmax function is used in the last fully connected layer. ReLU and softmax functions can each be expressed by (1) and (2), where K is the number of groups in the classifier.

$$f_1(x) = \begin{cases} x & , x \geq 0 \\ 0 & , x < 0 \end{cases} \quad (1)$$

$$f_2(x_i) = \frac{e^{x_i}}{\sum_{j=1}^K e^{x_j}} \quad (2)$$

Max-pooling is implemented between the convolutional layers. The operation only selects the maximum parameters from the pool. These decreases the number of parameters and computation in the network and therefore, control overfitting by progressively reducing the spatial size of the network. In the fully connected layer, the neurons have a complete connection to all the activations from the previous layers. The activations are computed with a matrix multiplication, followed by a bias offset. The number of convolutional and fully connected layers vary between CNN architectures. Figure 3 shows an example of the connections between the convolutional layers, activation functions, pooling, and fully connected layers.

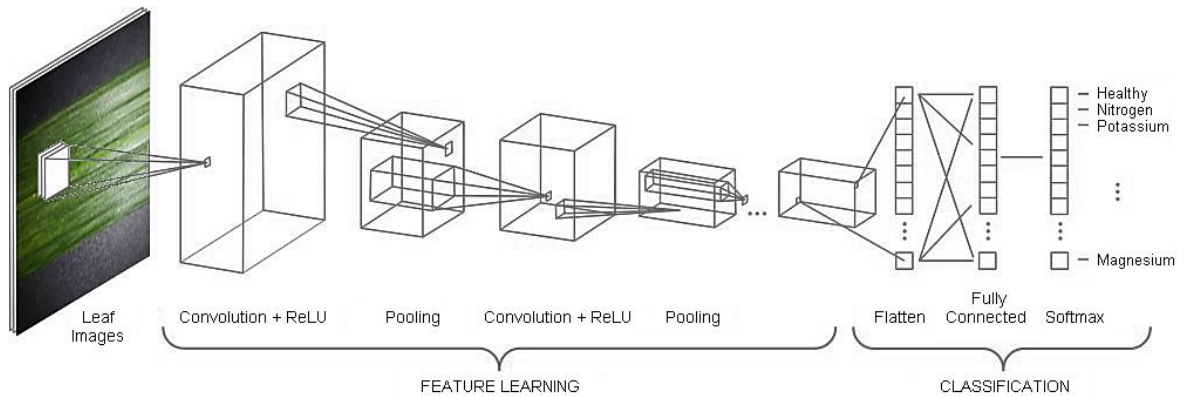


Figure 3. Example of connections between the convolutional layers, activation functions, pooling and fully connected layers

The study assesses four pre-trained modules that include ResNet-50, VGG-16, DenseNet201 and AlexNet architectures. The ResNet-50 is comprised of 49 convolutional layers and one fully connected layer. The first convolutional layer takes input image of 224×224 pixels. Meanwhile, VGG-16 consists of 13 convolutional layers and three fully connected layers. Similar with ResNet-50, the first convolutional layer takes in input image of 224×224 pixels. The DenseNet201 architecture has the deepest number of layers, comprising of 200 convolutional layers and one fully connected layer. The first convolutional layer also takes input image of 224×224 pixels. Conversely, AlexNet architecture has the least depth, consisting of five convolutional layers and three fully connected layers. The first convolutional layer takes in input image of 224×224 pixels.

The experiment runs on advanced micro devices (AMD) Ryzen 5 3400G with Radeon Vega Graphics processor, 32 GB random-access memory (RAM) and NVIDIA GeForce giga texel shader extreme (GTX) 1070 graphics processing unit (GPU) on Windows 10 operating system. Samples for the respective groups are initially randomized to avoid bias during classification. Then, the images are segregated for training and testing with 80:20 split ratio. A stochastic gradient descent algorithm is implemented for training the CNN. The randomized selection of data point from the set of data at each training iteration decreases the computation significantly [28]. At the end of training stage, the fully connected layers, softmax function and output layers for each architecture are replaced with the new layers that are developed for classifying leaves with nutrient deficiencies.

The performance of each architecture is assessed in terms of accuracy, specificity, sensitivity, and F-score. Accuracy represents the proportion of true positive (TP) and true negative (TN) results in the selected population. Meanwhile, recall is the ratio of TP that are correctly predicted by the classifier. Precision represents the probability that samples with positive classification that truly have the nutrient deficiency [29]. Specificity is the probability of the system predicting a particular class without giving false positive (FP) results [30]. Accuracy, recall, precision, and specificity are each presented by (3), (4), (5) and (6). FN denotes the false negative classifications. Meanwhile, F-score combines both recall and precision into a single measure that captures both properties. The parameter expressed by (7) is essentially the harmonic mean of the two fractions [31].

$$\text{Accuracy} = \frac{\text{TP} + \text{TN}}{\text{TP} + \text{TN} + \text{FP} + \text{FN}} \quad (3)$$

$$\text{Recall} = \frac{\text{TP}}{\text{TP} + \text{FN}} \quad (4)$$

$$\text{Precision} = \frac{TP}{TP + FP} \quad (5)$$

$$\text{Specificity} = \frac{TN}{TN + FP} \quad (6)$$

$$F - \text{score} = \frac{2 \times \text{Recall} \times \text{Precision}}{\text{Recall} + \text{Precision}} \quad (7)$$

3. RESULTS AND DISCUSSION

The results are presented in two sections. Initially, the discussion focuses on the features of healthy control, nitrogen-deficient, and potassium-deficient leaf images. This is then followed by the development of deep learning classification models using ResNet-50, VGG-16, DenseNet201 and AlexNet architectures. The performance of each CNN structure is compared based on accuracy, specificity, and F-score measures.

3.1. Acquisition of leaf images

A total of 180 leaf images were obtained based on the specified acquisition protocol. Equal number of samples have been acquired for healthy, nitrogen-deficient, and potassium-deficient leaves. Sample images for each class is shown in Figure 4. Notable features of nutrient deficiency can be observed. As shown in Figure 4(a), the colour of healthy leaves is dark green. Meanwhile, the nitrogen-deficient oil palm is presented by yellow-coloured leaflets in Figure 4(b). The potassium-deficient leaves shown in Figure 4(c) may be dark green, but with orange spots on the surface. The healthy leaves are used as control reference.

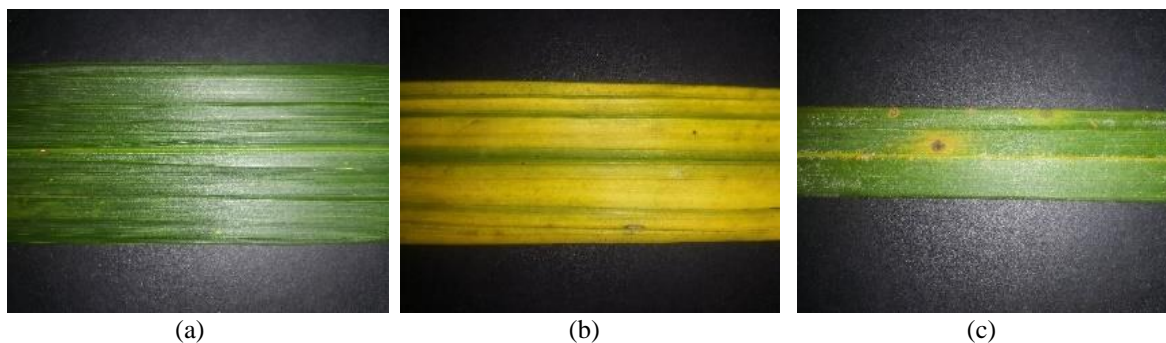


Figure 4. Sample images for (a) healthy control, (b) nitrogen-deficient, and (c) potassium-deficient leaves

3.2. Classification of nutrient deficiency using CNN

The leaf images were uploaded to the pre-trained CNN. Figure 5 shows the first convolutional weights for each architecture. Figure 5(a) refers to ResNet-50, Figure 5(b) represents VGG-16, Figure 5(c) is for DenseNet201, and Figure 5(d) represents AlexNet. The convolution process for each architecture shows different feature pattern being extracted from the same set of training images. These are then learned by the deeper network layers which combine the first convolution features to form the higher-level images.

All CNN architecture has attained training accuracies of 100%. Subsequently, each developed deep learning model is then tested using the remaining unseen images. VGG-16 and AlexNet has successfully yielded 100% testing accuracy, followed by DenseNet201 at 97.2%, and ResNet-50 at 94.4%. Confusion matrices for DenseNet201 and ResNet-50 are each shown by Table 1 and Table 2.

Based on the confusion matrices, it is evident that both architectures have misclassified images from potassium-deficient leaf as a healthy sample. These are attributed by the similar dark green-coloured leaves. Therefore, the size and distribution of yellow-coloured spotting on the surface of the leaves influences the capability of both architectures in the prediction process. Table 3 compares the performance of ResNet-50, VGG-16, DenseNet201 and AlexNet architectures using the overall classification accuracy, specificity, and F-score. The parameters consider the network performance during both training and testing.

By comparison, VGG-16 and AlexNet are the best performing architectures for classifying nutrient deficiency in oil palm from the leaf images. This is followed by DenseNet201 and subsequently, ResNet-50. Despite being trained with the same dataset, DenseNet201 and ResNet-50 were not able to perfectly classify

the unseen samples. Hence, both architectures are less efficient as they are comprised of significantly higher number of convolutional layers. Contrariwise, AlexNet presents the most viable solution with less complex network architecture. These supports the claim that VGG-16 is more computational costly than AlexNet in any classification problems [20].

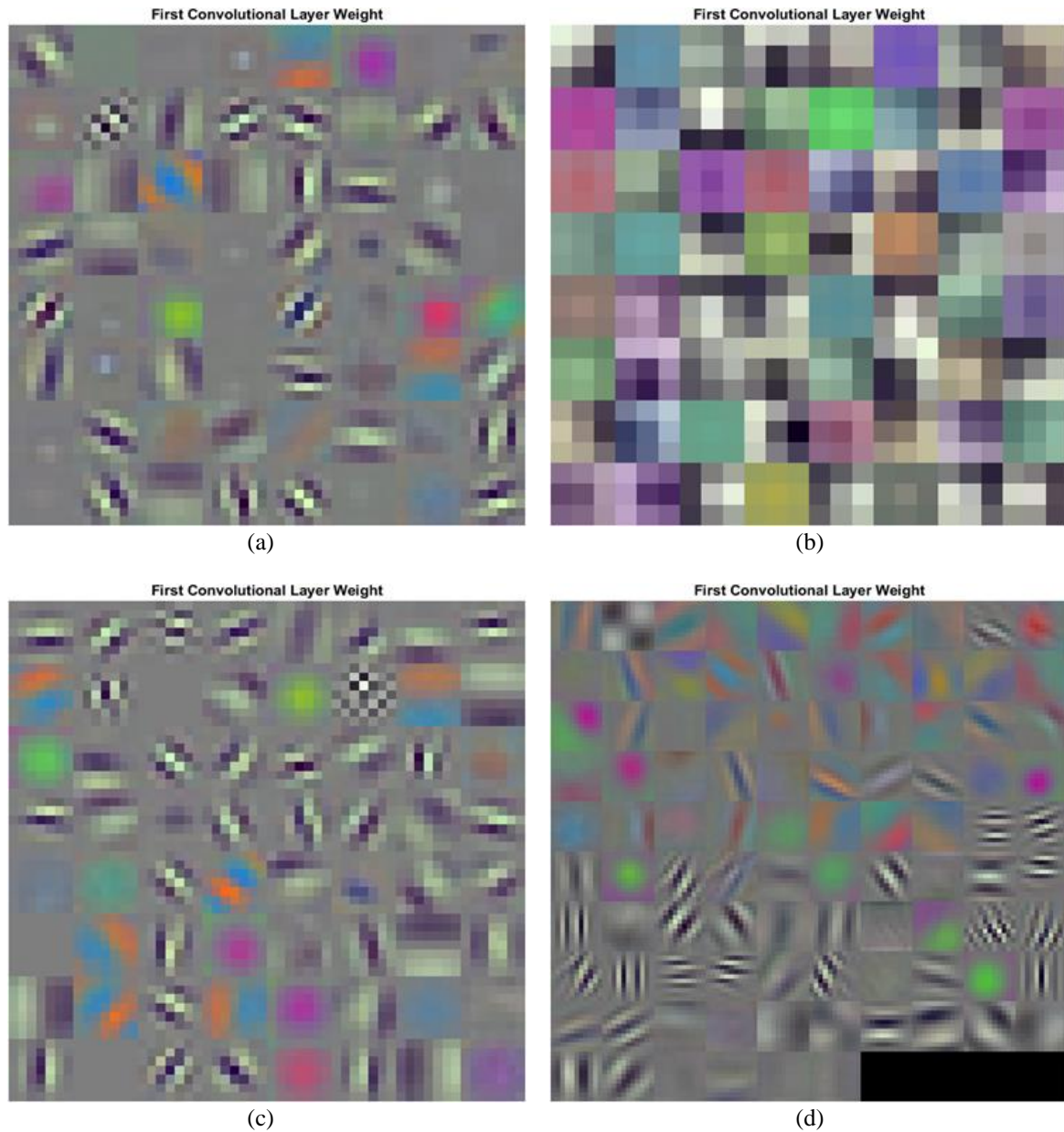


Figure 5. First convolutional layer weights for (a) ResNet-50, (b) VGG-16, (c) DenseNet-201, and (d) AlexNet

Table 1. Testing accuracy, recall and precision for DenseNet201

Nutrient Deficiency		Predicted			Recall (%)
		Healthy	Nitrogen	Potassium	
Target	Healthy	12	0	0	92.3
	Nitrogen	0	12	0	100
	Potassium	1	0	11	100
	Precision (%)	100	100	91.7	97.2

Table 2. Testing accuracy, recall and precision for ResNet-50

Nutrient Deficiency		Predicted			Recall (%)
		Healthy	Nitrogen	Potassium	
Target	Healthy	11	0	1	91.7
	Nitrogen	0	12	0	100
	Potassium	1	0	11	91.7
	Precision (%)	91.7	100	91.7	94.4

Table 3. Performance comparison between CNN architectures

Architecture	Accuracy (%)	Specificity (%)	F-score (%)
ResNet-50	96.7	99.4	98.9
VGG-16	100	100	100
DenseNet201	98.3	99.7	99.4
AlexNet	100	100	100

4. CONCLUSION

The study has initially set out to solve the following objectives: i) To establish a standard image acquisition protocol, and ii) To develop and assess CNN architectures for classifying nutrient deficiency from the leaf images. A standardized protocol for acquiring the leaf images has been successfully established. The acquired samples are validated by observing for characteristics of healthy, nitrogen-deficient, and potassium-deficient leaves. Subsequently, the images are used to develop deep learning classification models. The CNN architectures studied are ResNet-50, VGG-16, DenseNet201 and AlexNet. Overall, VGG-16 and AlexNet have demonstrated superior performance, yielding 100% accuracy for training and testing. Further inspection on the network structure indicates AlexNet as the more computational efficient architecture with less convolutional layers than VGG-16. Future improvement on the deep learning model includes expanding network capabilities to classify other classes of nutrient deficiencies. Furthermore, the proposed image acquisition protocol and use of smartphones hints at potential development of intelligent application for detecting nutrient deficiency from through the leaf images. These will reduce reliance on subjective evaluation of trained operators, thereby making the monitoring process more objective and efficient.

ACKNOWLEDGEMENTS

The work is supported by the Research Management Centre, Universiti Teknologi MARA through the LESTARI Grant (600-IRMI 5/3/LESTARI (032/2019)).




REFERENCES

- [1] A. Kushairi, R. Singh, and M. Ong-Abdullah, "The oil palm industry in Malaysia: Thriving with transformative technologies," *Journal of Oil Palm Research*, vol. 29, no. 4, pp. 431–439, Dec. 2017, doi: 10.21894/jopr.2017.00017.
- [2] A. S. A. F. Alam, A. C. Er, and H. Begum, "Malaysian oil palm industry: Prospect and problem," *Journal of Food, Agriculture & Environment*, vol. 13, no. 2, pp. 143–148, 2015.
- [3] P. Oettli, S. K. Behera, and T. Yamagata, "Climate based predictability of oil palm tree yield in Malaysia," *Scientific Reports*, vol. 8, no. 1, pp. 1–13, Feb. 2018, doi: 10.1038/s41598-018-20298-0.
- [4] A. M. Tarmizi and D. M. Tayeb, "Nutrient demands of Tenera oil palm planted on inland soils of Malaysia," *Journal of Oil Palm Research*, vol. 18, pp. 204–209, Jun. 2006.
- [5] I. Rankine and T. H. Fairhurst, "Management of phosphorus, potassium and magnesium in mature oil palm," *Better Crops International*, vol. 13, no. 1, pp. 10–15, May 1999.
- [6] G. W. Chapman and H. M. Gray, "Leaf analysis and the nutrition of the oil palm (*Elaeis guineensis* Jacq.)," *Annals of Botany*, vol. 13, no. 52, pp. 415–433, Oct. 1949, doi: 10.1093/oxfordjournals.aob.a083226.
- [7] S. Amalathas, A. Mitrovic, and S. Ravan, "Decision-making tutor: Providing on-the-job training for oil palm plantation managers," *Research & Practices in Technology Enhanced Learning*, vol. 7, no. 3, pp. 131–152, Nov. 2012.
- [8] N. A. Ali, S. A. Radzi, and A. S. Ja'afar, "Autism spectrum disorder classification on electroencephalogram signal using deep learning algorithm," *IAES International Journal of Artificial Intelligence (IJ-AI)*, vol. 9, no. 1, pp. 91–99, Mar. 2020, doi: 10.11591/ijai.v9.i1.pp91-99.
- [9] J. Schmidhuber, "Deep learning in neural networks: An overview," *Neural Networks*, vol. 61, pp. 85–117, Jan. 2015, doi: 10.1016/j.neunet.2014.09.003.
- [10] M. A. M. Azizi, M. N. M. Noh, I. Pasya, A. I. M. Yassin, and M. S. A. M. Ali, "Pedestrian detection using Doppler radar and LSTM neural network," *IAES International Journal of Artificial Intelligence (IJ-AI)*, vol. 9, no. 3, pp. 394–401, Sep. 2020, doi: 10.11591/ijai.v9.i3.pp394-401.
- [11] R. B. Roslan, I. N. M. Razly, N. Sabri, and Z. Ibrahim, "Evaluation of psoriasis skin disease classification using convolutional neural network," *IAES International Journal of Artificial Intelligence (IJ-AI)*, vol. 9, no. 2, pp. 349–355, Jun. 2020, doi: 10.11591/ijai.v9.i2.pp349-355.
- [12] K. He, X. Zhang, S. Ren, and J. Sun, "Deep residual learning for image recognition," in *2016 IEEE Conference on Computer Vision and Pattern Recognition (CVPR)*, Jun. 2016, pp. 770–778, doi: 10.1109/cvpr.2016.90.




- [13] K. Simonyan and A. Zisserman, "Very deep convolutional networks for large-scale image recognition," in *3rd International Conference on Learning Representations*, 2015, pp. 1–14, doi: 10.48550/arXiv.1409.1556.
- [14] G. Huang, Z. Liu, L. Van Der Maaten, and K. Q. Weinberger, "Densely connected convolutional networks," in *2017 IEEE Conference on Computer Vision and Pattern Recognition (CVPR)*, Jul. 2017, pp. 4700–4708, doi: 10.1109/cvpr.2017.243.
- [15] A. Krizhevsky, I. Sutskever, and G. E. Hinton, "ImageNet classification with deep convolutional neural networks," *Communications of the ACM*, vol. 60, no. 6, pp. 84–90, May 2017, doi: 10.1145/3065386.
- [16] B. S. A. Gazioglu and M. E. Kamaşak, "Effects of objects and image quality on melanoma classification using deep neural networks," *Biomedical Signal Processing and Control*, vol. 67, p. 102530, May 2021, doi: 10.1016/j.bspc.2021.102530.
- [17] V. Tiwari, R. C. Joshi, and M. K. Dutta, "Dense convolutional neural networks based multiclass plant disease detection and classification using leaf images," *Ecological Informatics*, vol. 63, p. 101289, Jul. 2021, doi: 10.1016/j.ecoinf.2021.101289.
- [18] K. K. Bressemer, L. C. Adams, C. Erxleben, B. Hamm, S. M. Niehues, and J. L. Vahldiek, "Comparing different deep learning architectures for classification of chest radiographs," *Scientific Reports*, vol. 10, no. 1, pp. 1–16, Aug. 2020, doi: 10.1038/s41598-020-70479-z.
- [19] M. Lv, G. Zhou, M. He, A. Chen, W. Zhang, and Y. Hu, "Maize leaf disease identification based on feature enhancement and DMS-robust Alexnet," *IEEE Access*, vol. 8, pp. 57952–57966, Mar. 2020, doi: 10.1109/access.2020.2982443.
- [20] I. Khandelwal and S. Raman, "Analysis of transfer and residual learning for detecting plant diseases using images of leaves," in *Advances in Intelligent Systems and Computing*, Springer Singapore, 2018, pp. 295–306.
- [21] T. T. Nguyen *et al.*, "Monitoring agriculture areas with satellite images and deep learning," *Applied Soft Computing*, vol. 95, p. 106565, Oct. 2020, doi: 10.1016/j.asoc.2020.106565.
- [22] P. Nevavuori, N. Narra, and T. Lipping, "Crop yield prediction with deep convolutional neural networks," *Computers and Electronics in Agriculture*, vol. 163, p. 104859, Aug. 2019, doi: 10.1016/j.compag.2019.104859.
- [23] S. Tu *et al.*, "Passian fruit detection and counting based on multiple scale faster R-CNN using RGB-D images," *Precision Agriculture*, vol. 21, no. 5, pp. 1072–1091, Jan. 2020, doi: 10.1007/s11119-020-09709-3.
- [24] H. Jiang, C. Zhang, Y. Qiao, Z. Zhang, W. Zhang, and C. Song, "CNN feature based graph convolutional network for weed and crop recognition in smart farming," *Computers and Electronics in Agriculture*, vol. 174, p. 105450, Jul. 2020, doi: 10.1016/j.compag.2020.105450.
- [25] S. K. Noon, M. Amjad, M. A. Qureshi, and A. Mannan, "Use of deep learning techniques for identification of plant leaf stresses: A review," *Sustainable Computing: Informatics and Systems*, vol. 28, p. 100443, Dec. 2020, doi: 10.1016/j.suscom.2020.100443.
- [26] B. Jiang *et al.*, "Fusion of machine vision technology and AlexNet-CNNs deep learning network for the detection of postharvest apple pesticide residues," *Artificial Intelligence in Agriculture*, vol. 1, pp. 1–8, Mar. 2019, doi: 10.1016/j.iiia.2019.02.001.
- [27] J. Sun, W. Tan, H. Mao, X. Wu, Y. Chen, and L. Wang, "Recognition of multiple plant leaf diseases based on improved convolutional neural network," *Transactions of the Chinese Society of Agricultural Engineering*, vol. 33, no. 19, pp. 209–215, Oct. 2017.
- [28] H. Robbins and S. Monro, "A stochastic approximation method," *The Annals of Mathematical Statistics*, vol. 22, no. 3, pp. 400–407, Sep. 1951, doi: 10.1214/aoms/1177729586.
- [29] A. H. Jahidin *et al.*, "Classification of intelligence quotient using EEG sub-band power ratio and ANN during mental task," in *2013 IEEE Conference on Systems, Process & Control (ICSPC)*, Dec. 2013, pp. 204–208, doi: 10.1109/spc.2013.6735132.
- [30] W. Zhu, N. Zeng, and N. Wang, "Sensitivity, specificity, accuracy, associated confidence interval and ROC analysis with practical SAS® implementations," in *NESUG Proceedings: Health Care and Life Sciences*, 2010, pp. 1–9.
- [31] Q. Song, H. Jiang, and J. Liu, "Feature selection based on FDA and F-score for multi-class classification," *Expert Systems with Applications*, vol. 81, pp. 22–27, Sep. 2017, doi: 10.1016/j.eswa.2017.02.049.

BIOGRAPHIES OF AUTHORS







Muhammad Ikmal Hafiz Razali    received his B.Eng. (Electronics) from Universiti Teknologi MARA, Malaysia in 2020. He is currently an engineer at Mindmatics Sdn. Bhd. His main research interest is in deep learning for agriculture applications. He can be contacted at email: m.ikmalhafiz17@gmail.com.







Muhammad Asraf Hairuddin    received his PhD in Electrical Engineering from Universiti Teknologi MARA, Malaysia, in 2014. He is currently a senior lecturer at the College of Engineering, Universiti Teknologi MARA Cawangan Johor, Malaysia. His research interests include image processing, artificial intelligence, and deep learning applications. He can be contacted at email: masraf@uitm.edu.my.







Aisyah Hartini Jahidin     received her B.Eng. (Telecommunication) and M.Eng.Sc. (Magnetic Materials) from University of Malaya, Malaysia, in 2002 and 2006, respectively. She obtained her Ph.D. in Electrical Engineering from Universiti Teknologi MARA, Malaysia, in 2015. She is also a senior member of the Institute of Electrical and Electronics Engineers. She is currently a senior lecturer for the Centre for Foundation Studies in Science, University of Malaya, Malaysia. Her main research interests include biomedical signal processing, psychometric assessments, and machine learning applications. She can be contacted at email: aisyah23@um.edu.my.



Mohd Hanafi Mat Som     received his Bachelor's and Master's degree in Biomedical Engineering from University of Malaya, Malaysia, in 2006, and University of New South Wales, Australia, in 2008. He was then awarded with Doctor of Engineering in System Design Engineering from University of Fukui, Japan, in 2015. He is also a professional technologist (P.Tech) in Electrical and Electronic Technology, registered with the Malaysia Board of Technologists, Malaysia. He is currently a senior lecturer at the Faculty of Electronic Engineering Technology, Universiti Malaysia Perlis. He is also an associate fellow at the Sport Engineering Research Centre, Universiti Malaysia Perlis. His research interests include image processing and artificial intelligence. He can be contacted at email: mhanafi@unimap.edu.my.



Megat Syahirul Amin Megat Ali     received his B.Eng. (Biomedical) from University of Malaya, Malaysia, in 2006. He then obtained M.Sc. in Biomedical Engineering from University of Surrey, United Kingdom, in 2007. He received his Ph.D. in Electrical Engineering from Universiti Teknologi MARA, Malaysia, in 2018. He is a chartered engineer (C.Eng.), registered with the Engineering Council, United Kingdom, and senior member of the Institute of Electrical and Electronics Engineers. He is currently a research fellow at Microwave Research Institute, Universiti Teknologi MARA, Malaysia. His main research interests include biomedical signal processing, and applications of machine learning for solving engineering problems. He can be contacted at email: megatsyahirul@uitm.edu.my.